Three-dimensional wave-based simulation of outdoor sound propagation using the constrained interpolation profile method with a variable-grid technique

Takashi ISHIZUKA[1]; Kan OKUBO[2]

[1] Institute of Technology, Shimizu Corporation, Japan

[2] Graduate School of System Design, Tokyo Metropolitan University, Japan

ABSTRACT

In the present report, a variable-grid technique for the CIP (constrained interpolation profile) method is applied to three-dimensional wave-based simulation of sound propagation in an outdoor field. This technique is based on the sub-grid technique and provides a procedure for dynamic setting of subgridded areas according to wave propagation to achieve high accuracy with low computational costs. The effectiveness of proposed technique is examined in a practical outdoor field including a complex topography and a building. Sound propagation in the three-dimensional outdoor field and how the subgridded areas follow waves are visualized and shown. The examinations reveal that proposed technique has almost the same accuracy with that the normal CIP simulation with a finer uniform-grid system has. Also, the simulation applying the variable-grid system requires about one-fourth of computer memory and one-fifth of computational time relative to those the normal finer simulation requires.

Keywords: Outdoor sound propagation, Sound field analysis, CIP method, Variable grid, Numerical diffusion
I-INCE Classification of Subjects Number: 76.9

1. INTRODUCTION

The constrained interpolation profile (CIP) method was developed in the field of fluid dynamics as a kind of the method of characteristics (MOC)(1, 2). This method has been applied to numerical simulations of sound field in time domain(3, 4, 5) as it has an advantage of low numerical dispersion over the finite-difference time-domain (FDTD) method widely used for sound field analysis. Additionally, a spatial grid size and a time step size which the CIP method requires for adequate accuracy are larger than those the FDTD method requires. In the CIP method, a time step size is free from Courant condition. The CIP method does not require a small time step size for stability, resulting in a reduction of total computational time.

However, results of CIP simulations involve errors due to numerical diffusion. Attenuation of sound waves with their propagation exceeds physical phenomena, e.g. geometrical attenuation. These errors are unignorable in calculations of sound propagation in large-scale sound fields such as an outdoor field. To divide calculated field with smaller grid size can reduce these errors. However, it increases the number of grids and results in significant increase of computational time and required memory.

We have proposed a variable-grid technique for the CIP method to accurately calculate sound fields with low computational costs(5). This technique is based on the sub-grid technique for the CIP method (6) and provides a procedure for dynamic setting of subgridded areas according to wave propagation. The effectiveness of proposed method was confirmed in basic examinations in a two-dimensinal free field(5). This report shows examinations of the CIP simulation with the variable-grid technique in a three-dimensional sound feild. A practical outdoor field is assumed for the examinations. Sound propagation in the field including a complex topography and a building is calculated using proposed method.

2. NUMERICAL METHOD

2.1 CIP method

The CIP method for acoustic simulation computes advection equations derived from the governing equations of sound fields. The equation of continuity and the equation of motion for a lossless linear sound field

[1] ishiduka@shimz.co.jp

are transformed into

$$\partial_t p + cZ\partial_x v_x = 0, \quad Z\partial_t v_x + c\partial_x p = 0, \tag{1}$$

where ∂_α represents an operator $\partial/\partial\alpha$, and p, v_x, c, and Z are the sound pressure, the particle velocity in the x-direction, the speed of sound, and the characteristic impedance of a medium, respectively. Addition and subtraction of the two equations in Eq. (1) derive the following advection equations:

$$\partial_t f_{x\pm} \pm c\partial_x f_{x\pm} = 0, \text{ for } f_{x\pm} = p \pm Zv_x. \tag{2}$$

f_{x+} and f_{x-} represent forward and backward components of the sound field in the x-direction and Eq. (2) expresses propagation of them with the velocity of c.

In the MOC, the advection equations expressing wave propagation are computed by advection calculations schematically illustrated in Fig. 1. As shown in the diagram, advecting $f_{x\pm}$ at points $\mp c\Delta t$ distant from a grid point x_i at a time step n gives those at x_i at the next time step:

$$f_{x\pm}^{n+1}(x_i) = f_{x\pm}^{n}(x_i \mp c\Delta t), \tag{3}$$

where Δt is the time step size, and the superscripts n and $n+1$ denote time steps. When the points $x_i \mp c\Delta t$, called advection sources, are not at grid points, $f_{x\pm}^{n}(x_i \mp c\Delta t)$ are obtained by using interpolations.

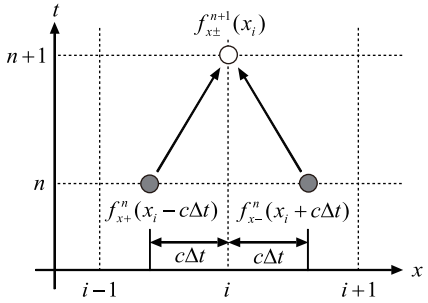

Figure 1 – Advection of values in the method of characteristics.

In the CIP method, a kind of the MOC, values at advection sources are interpolated with high accuracy by using the Hermite interpolation(1), normally the 3rd-order Hermite interpolation. These calculations need spatial derivatives of $f_{x\pm}$ at each grid. Advection equations for the derivatives are derived from the differentiation of Eq. (2):

$$\partial_t g_{x\pm} \pm c\partial_x g_{x\pm} = 0, \text{ for } g_{x\pm} = \partial_x p \pm Z\partial_x v_x = \partial_x f_{x\pm} \tag{4}$$

The CIP method simultaneously computes Eq. (2) and (4) using the 3rd-order Hermite interpolation.

The above formulation expresses one-dimensional wave propagation in the x-direction. Multi-dimensional wave propagation is computed by the directionally separated advection formulation, where one-dimensional advections for each axis are alternately computed. This technique requires additional advection calculations for spatial derivatives with respect to the direction perpendicular to the advection direction. For the x-directional advection in a three-dimensional field, $\partial_y f_{x\pm}$, $\partial_y g_{x\pm}$, $\partial_z f_{x\pm}$, $\partial_z g_{x\pm}$, $\partial_y\partial_z f_{x\pm}$, and $\partial_y\partial_z g_{x\pm}$ are taken into calculation. Advection equations for these perpendicular derivatives are derived from the differentiation of Eq. (2) and Eq. (4) and computed simultaneosly. The type-C CIP method is employed in this report, where the perpendicular derivatives at the advection sources are also calculated by using the 3rd-order Hermite interpolation(2, 3). We can calculate the y-directional and the z-directional advections in a similar procedure to that for the x-direction described above. Results of sequential advections in the x-, the y-, and the z-direction are asigned to the vales at the next time step.

2.2 Variable-grid technique

The variable-grid technique proposed here is based on the sub-grid technique. In the sub-grid technique, a calculated field is divided into multiple-sized grids, where the coarse grid sizes is Δl ($= \Delta x = \Delta y = \Delta z$), and the fine grid sizes in a subgridded area is Δl_s ($\Delta l_s = \Delta l/N$, $N = 2, 3, \ldots$). To suppress errors due to the numerical diffusion the CIP method involves, we apply the sub-grid technique to areas where the physical values widely fluctuate. These area will shift according to wave propagation. Therefore, subgridded areas are dynamically set through the following procedure.

- Before starting calculations, divide the sound field into blocks including a number of coarse grids, normally cubic blocks of the same size.

- One of the physical values and their derivatives is specified as an evaluation value. During calculations, if an absolute value of the evaluation value at any point in a coarse-grid block exceeds a given threshold, divide the block into the finer grids, i.e. convert the block to a subgridded block. As shown in Fig. 2, derive the physical values and their derivatives at newly defined points (open circles) from those at existing points (gray circles) by using the 3rd-order Hermite interpolation.
- Meanwhile, if absolute values of the evaluation values at all points in a subgridded block fall below the given threshold, reintegrate the finer grids into the original coarse grids. Extract the physical values and their derivatives at coarse-grid points, and discard the others.

In the coarse-grid and subgridded areas, advection calculations are similarly carried out using the grid sizes of each area. However, calculations at an interface between these areas need an additional treatment (6). Figure 3 schematically illustrates the procedure for advection calculations in the $+x$-direction at the edge of the subgridded area, for example. The first step is to interpolate f_{x+}, g_{x+}, and thier perpendicular derivatives at the point indicated by the open square in Fig. 3 from the values at the coarse-grid points using the 3rd-order Hetmite interpolation. Using the values at the coarse-grid points and interpolated values at the open square point enables the advection calculations for all the points at the edge of the subgridded area. That is, to interpolate the values at the points $c\Delta t$ distant from the edge of the subgridded area, and to advect them.

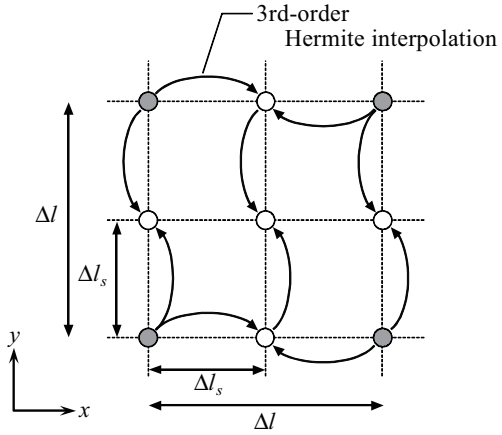

Figure 2 – Interpolation of values at sub-grid points from coarse-grid points.

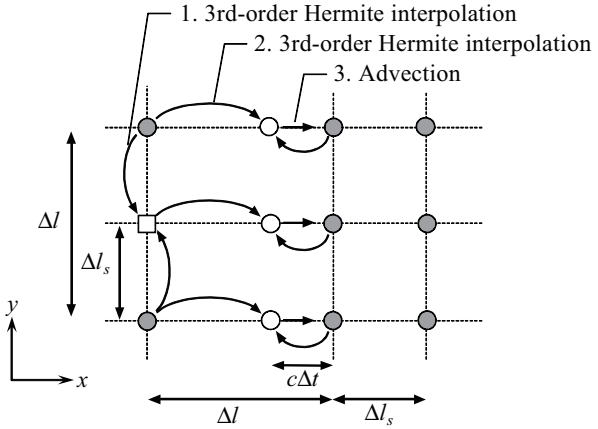

Figure 3 – Advection calculation at an interface between coarse-grid and subgridded areas.

2.3 Boundary condition

In the CIP method, boundary conditions at the interface between two media are given using the reflection coefficient. When f_{x+} and g_{x+} are incident on the boundary at x_b, for example, the boundary conditions are represented as

$$f_{x-}(x_b) = \Gamma f_{x+}(x_b), \tag{5}$$

$$g_{x-}(x_b) = \Gamma' g_{x+}(x_b). \tag{6}$$

Γ denotes the reflection coefficient of p and v_x and Γ' denotes that of the spatial derivatives $\partial_x p$ and $\partial_x v_x$, respectively. The Dirichlet and Neumann conditions on the boundary give the following relation:

$$\Gamma' = -\Gamma. \tag{7}$$

We can explicitly give the reflection coefficients Γ and Γ' as constants as long as they satisfy Eq. (7). For example, $\Gamma = 1$ and $\Gamma' = -1$ are set to a perfectly reflective surface.

In multi-dimensional simulations, boundary conditions for the perpendicular derivatives are given in similar forms to Eqs. (5) and (6) as a result of spatial differentiations of these equations.

3. NUMERICAL RESULTS AND DISCUSSIONS

We show numerical results of sound propagation in a three-dimensional outdoor field calulated by proposed method, and compare accuracy and efficiency of the varible-grid system with those of the conventional uniform-grid system. Figure 4 shows caluclated sound field. We assume a site of a factory including a part of a building and a residential zone beyond an embankment. Calculation parameters are as follows: the coarse-grid sizes are $\Delta l = 0.3$ m; the sub-grid sizes are $\Delta l_s = 0.1$ m, i.e. $N = 3$; the time step size is $\Delta t = 1.0 \times 10^{-4}$ s; the speed of sound is $c = 343.4$ m/s. The field is divided into $25 \times 25 \times 10$ blocks and each block includes $8 \times 8 \times 8$ coarse grids. The threshold for converting a coarse-gird block to a subgridded block is the sound pressure of 0.5×10^{-3}. All boundaries assumed to be perfectly reflective, i.e. $\Gamma = 1$ and $\Gamma' = -1$. Additionally, the PML(7, 8) with 16 layers surrounds calculated field except the outer boundary in the $-z$-direction. The attenuation parameter of the PML is $R = 1.4\rho c$. In the PML region, the grid size is fixed at the coarse-grid size for simplicity of a calculation. A point source is set at $(x_c, y_c, z_c) = (6, 30, 0)$ as shown in Fig. 4. The initial sound pressure distribution is given as the Gaussian with the unit amplitude:

$$p(x,y) = \exp\left\{-\frac{(x-x_c)^2 + (y-y_c)^2 + (z-z_c)^2}{2 \cdot 0.4^2}\right\}. \tag{8}$$

The initial distributions of spatial derivatives of p are also given as the differentiations of Eqn. 8.

For comparisons, the same sound field is calculated by uniform-grid systems with $\Delta l = 0.3$ m and $\Delta l = 0.1$ m (hereafter, the coarse- and the fine-grid systems, respectively). The grid size of the latter is equal to the sub-grid size of the variable-grid system.

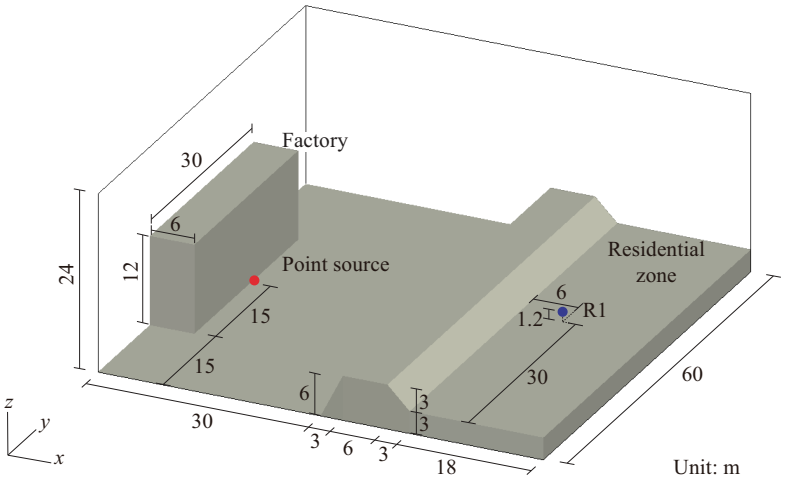

Figure 4 – Calculated sound field.

Figure 5 shows sound pressure distributions in a xz-virtical plane including the source point and horizontal planes 0.3 m above the ground level at $t = 200\Delta t, 600\Delta t, 1\,000\Delta t$, and $1\,400\Delta t$. Green squares in Fig. 5 represent subgridded blocks with finer grids. It is confirmed that the variable-grid technique can dynamically set subgridded areas accorgind to wave propagation. The subgridded areas follow main wave fronts of reflected and diffracted waves as well as the direct wave. Meanwhile, areas where the amplitude of wave fronts is smaller than the threshold remain coarse-grid areas.

Figure 6 compares sound pressure trasients calculated by the variable-grid, the fine-grid, and the coarse-grid systems at the point R1: (48, 30, 4.2) shown in Fig. 4. In the result of the coarse-grid system, suppression of amplitude caused by the numerical diffusion is observed. In contrast, the result of the varible-grid system

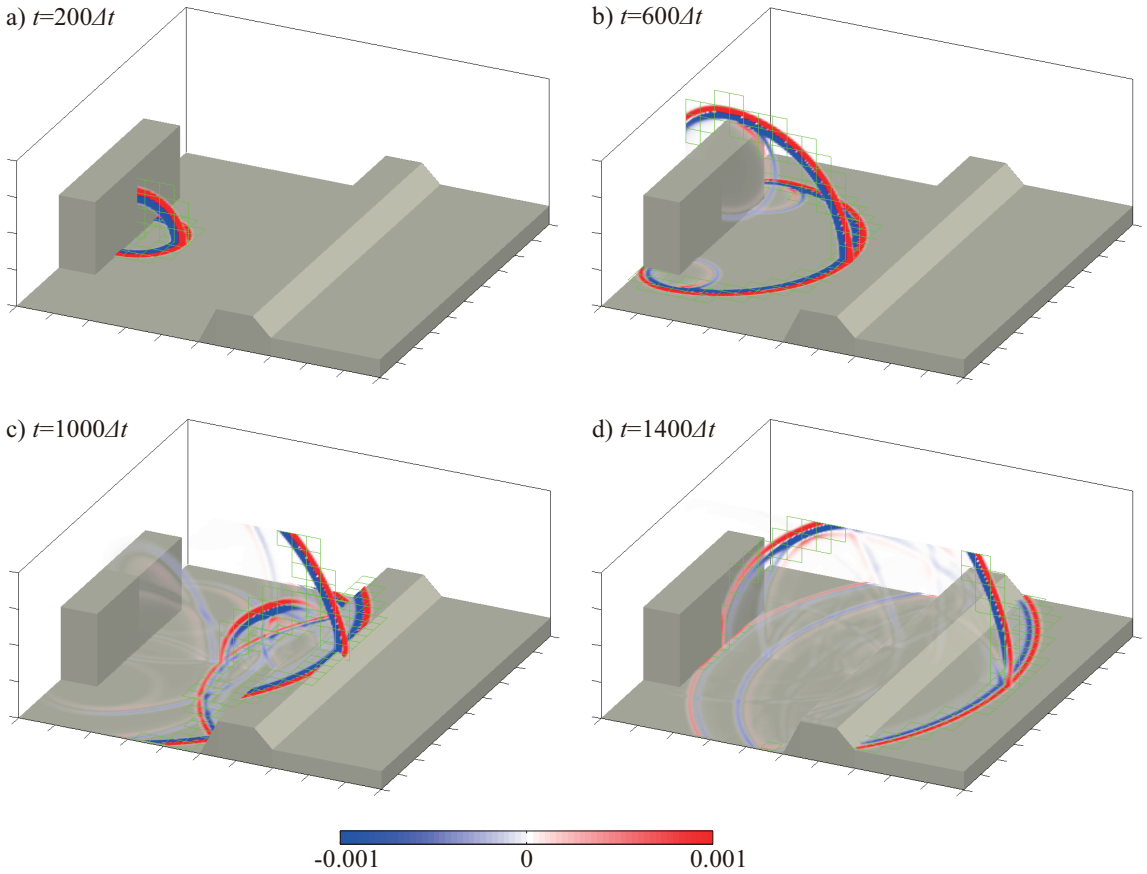

Figure 5 – Sound pressure distributions at $t = 200\Delta t, 600\Delta t, 1\,000\Delta t$, and $1\,400\Delta t$ ($\Delta t = 1.0 \times 10^{-3}$). Green squares represent subgridded blocks with finer grids.

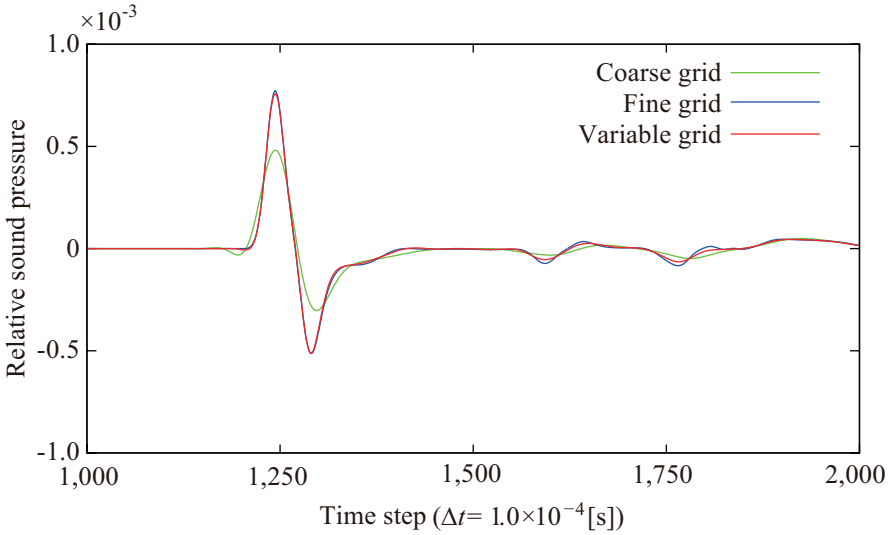

Figure 6 – Sound pressure transients at the point R1: (48, 30, 4.2) calculated by the variable-grid, the fine-grid, and the coarse-grid systems.

well agrees with that of the fine-grid system. This means that the variable-grid technique can reduce the errors due to the numerical diffusion. After $t = 1\,500\Delta t$, the results of the varible-grid system slightly differs from that of the fine-grid system. Waves with amplitude smaller than the threshold are not followed by the subgridded area as described above. Therefore, these small waves are suppressed a little by the numerical diffusion.

Figure 7 shows the number of grids in the calculation with the varible-grid system at each time step as ratios relative to that the fien-grid system requires. At the beginning of the calculation, the number of grids increases with increase of the number of subgridded blocks according to the spread of the wave fronts. After the wave fronts reache at the end of the calculated field, the number of grids decreases gradually. The maximum number of grids is 26% of the fine-grid system. Table 1 compares computational costs of the variable-grid system and the uniform-grid systems. It is found that the variable-grid system requires about one-fourth of computer memory and one-fifth of computational time relative to those the fine-grid system requires.

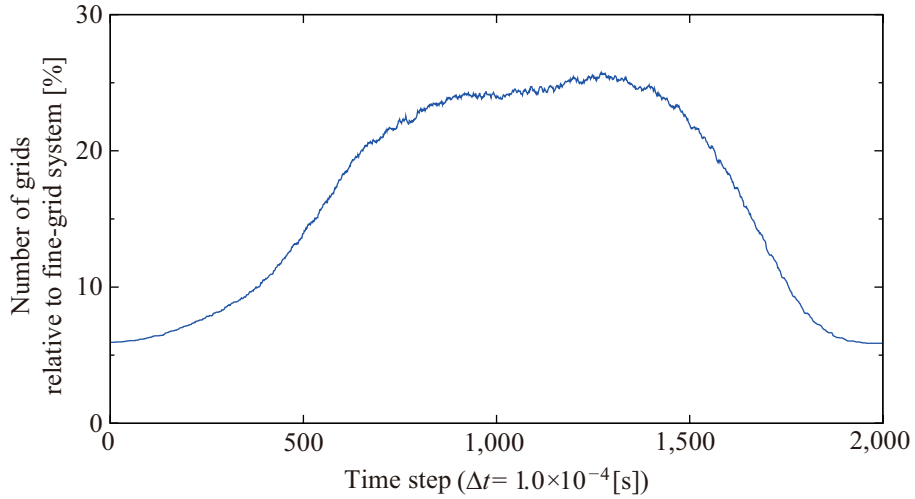

Figure 7 – Number of grids in the varible-grid system calculation at each time step as ratios relative to that the fien-grid system requires.

Table 1 – Computational costs of the varible-grid, the fine-grid, and the coarse-grid systems. Percentages in parentheses are ratio relative to the fine-grid system.

Grid system	Maximum number of grids	Calculation time [s]
Fine	82.24 $\times 10^6$ (100%)	48.23 $\times 10^3$ (100%)
Coarse	4.81 $\times 10^6$ (5.9%)	4.47 $\times 10^3$ (9.3%)
Variable	21.18 $\times 10^6$ (25.8%)	9.49 $\times 10^3$ (19.7%)

4. CONCLUSIONS

In this report, the CIP method with the variable-grid technique is applied to numerical simulation of three-dimensional outdoor sound field. This technique provides the procedure for dynamic setting of subgridded areas according to wave propagation. The examination assuming a practical outdoor field revealed the followings:

- The variable-grid technique achieves almost the same accuracy with the finer uniform-gird system reducing the errors due to the numerical diffusion.
- The variable-grid technique reduces computational costs. The simulation using this technique requires about one-fourth of computer memory and one-fifth of computational time relative to those required in the simulation using the finer uniform-grid.

REFERENCES

1. Yabe T, Xiao F, Utsumi T. Constrained interpolation profile method for multiphase analysis. J Comput Phys. 2001;169:556–593.

2. Aoki T. Multi-dimensional advection of cip (cubic interpolated propagation) scheme. Comput Fluid Dynamics J. 1995;4:279–291.

3. Konno M, Okubo K, Tsuchiya T, Takeuchi N. Performance of various types of constrained interpolation profile method for two-dimensional numerical acoustic simulation. Jpn J Appl Phys. 2008;47:3962–3963.

4. Tachioka Y, Yasuda Y, Sakuma T. Application of the constrained interpolation profile method to room acoustic problems: Examination of boundary modeling and spatial/time discretization. Acoust Sci & Tech. 2012;33:22–32.

5. Ishizuka T, Okubo K, Ara Y. Variable-grid technique for sound field analysis using the constrained interpolation profile method. Acoust Sci & Tech. 2012;33:387–390.

6. Ara Y, Okubo K, Tagawa N, Tsuchiya T, Ishizuka T. Examination of sub-grid technique for simulation of sound wave propagation using constrained interpolation profile method with method of characteristics. Jpn J Appl Phys. 2011;50:07HC20.

7. Ando Y, Hayakawa M. Implementation of the perfectly matched layer to the cip method. IEICE Trans Electron. 2006;p. E98–C:645–648.

8. Ishizuka T, Okubo K. Formulation and examination of the perfectly matched layer for sound field analysis using the constrained interpolation profile method. Acoust Sci & Tech. 2013;34:378–381.